Finite Temperature Structure and Dynamics of Zinc Dialkyldithiophosphate Wear Inhibitors: A Density Functional Theory and ab Initio Molecular Dynamics Study

Nicholas J. Mosey and Tom K. Woo*

Department of Chemistry, The University of Western Ontario, London, Ontario, Canada N6A 5B7

Received: January 13, 2003; In Final Form: April 21, 2003

The thermal decomposition of several zinc dialkyldithiophosphate (ZDDP) antiwear additives has been explored with both finite temperature gas-phase ab initio molecular dynamics (MD) simulations and static quantum chemical calculations at the density functional (DFT) level of theory. Calculations have been performed on the ZDDP monomers ($Zn(S_2P(OR)_2)_2$), ZDDP dimers, and the corresponding linkage isomers (LI-ZDDPs) with a variety of substituents (R = H, Me, Et, ^{i}Pr, ^{t}Bu, Ph). The results show that the monomeric form of ZDDP likely dominates at finite temperatures for all substituents considered and that the LI-ZDDP isomer is nearly thermoneutral with respect to the parent ZDDP monomer. Optimized geometries of the ZDDP monomer give 4-coordinate Zn structures that are consistent with previously reported theoretical calculations. However, ab initio molecular dynamics simulations of the ZDDP monomers at elevated temperatures show that 2- and 3-coordinate complexes are instead favored and that the decrease in coordination number has a significant effect on the electronic structure of the molecule that may affect the reactivity of ZDDPs with other chemical species present in engine oils. The ab initio MD simulations also provide insight into several decomposition pathways of the various ZDDP species that include the loss of either alkyl or alkoxy radicals as well as the elimination of olefins and sulfides from the ZDDP molecule. The results are discussed in terms of how the observed processes will affect the overall abilities of the antiwear film.

I. Introduction

Zinc dialkyldithiophosphates (ZDDPs) have been employed as additives in commercial motor oils for over 50 years due to their amazing antiwear properties,[1−4] and to date no superior alternative has been found. Given the great importance and utility of ZDDP additives, and the antiwear films derived from them, numerous studies have taken place in hopes of developing a clear description of the process of film formation and acquiring an understanding of the fundamental nature of the properties that these films exhibit.[1,5−14] Although a large amount of attention has been devoted to exploring ZDDP film formation, many questions remain unanswered,[15,16] in part due to the difficulties encountered upon examining the formation of antiwear films under engine conditions or similar conditions in the lab.[17,18] Furthermore, the multidisciplinary nature of the study of ZDDP molecules and films complicates this task,[19] and there remains an obvious need to develop a model for the behavior of ZDDPs that is consistent with the wealth of available experimental data in order to optimize their effectiveness in current motor oils. It has also recently become apparent that atomic level knowledge of the formation of ZDDP films is necessary to develop alternative antiwear additives to meet environmental standards[20,21] and for the effective use on materials other than steel, particularly aluminum.[22,23]

It is generally accepted that ZDDPs decompose under normal engine conditions and that the decomposition products form polyphosphate chains that interconnect and grow forming "pads" on engine parts that act as sacrificial riding surfaces, undergoing wear as a result of friction to protect the underlying material.[18,24−27] Although thermal, or thermooxidative, decomposition is regarded as the major mechanism of antiwear film formation, the specific steps involved in this process remain unclear.[17,28,29] Additionally, the interaction of ZDDP molecules with other species present in the oil, such as peroxides, acids, and water, and the engine surface itself, are not well understood.[30−32]

The general structure of the monomeric form of ZDDP is shown in Figure 1a. It was established long ago that the products of the thermal decomposition of this molecule, as well as its higher order oligomers, include a variety of volatile and oil-soluble species such as olefins, mercaptans, and sulfides as well as insoluble phosphorus-containing species that are thought to be the building blocks of the polyphosphate antiwear film.[33] A mechanism to describe the formation of these products through the thermal decomposition of ZDDP molecules in solution has been proposed[34] involving the initial acid-catalyzed isomerization of the ZDDP molecule through the transfer of one or more alkyl groups from an oxygen atom to a sulfur atom. The resulting species, referred to as a linkage isomer of ZDDP (LI-ZDDP), shown in Figure 1b, was proposed to undergo further decomposition yielding olefins through the transfer of a β-hydrogen from the alkyl group to the dealkylated oxygen atom while sulfur-containing species are formed through the acid-catalyzed loss of thiols that then react to form mercaptans and sulfides. The resulting phosphorus-containing products were proposed to be (thio)phosphate-like structures, with zinc acting as the cation, that undergo subsequent polymerization to form a glassy polyphosphate film.

Using data obtained through ^{1}H and ^{31}P NMR studies of the thermal decomposition of ZDDPs in white oil combined with the chemical processes that thiophosphate esters are reported to take part in, a different mechanism has been proposed[35,36]

* To whom correspondence should be addressed. E-mail: twoo@uwo.ca.

10.1021/jp034085c CCC: $25.00
Published on Web 06/04/2003

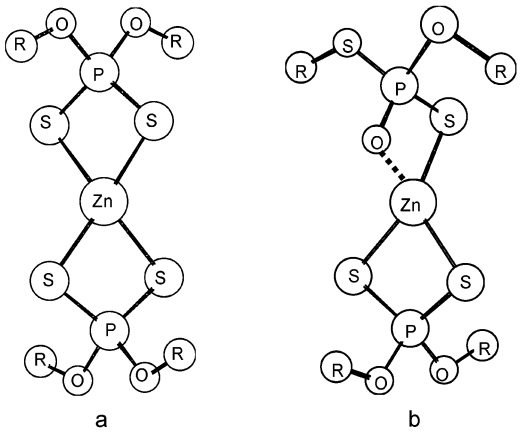

Figure 1. (a) ZDDP monomer. (b) LI-ZDDP monomer. In this study "R" refers to hydrogen (H), methyl (Me), ethyl (Et), isopropyl (^{i}Pr), *tert*-butyl (^{t}Bu), or phenyl (Ph) substituents.

that accounts for the formation of olefins and volatile sulfur-containing products as well as oil-soluble trialkyltetrathiophosphates ($S{=}P(SR)_3$) and insoluble polyphosphate-like species that form the antiwear pad. This mechanism also involves the initial rearrangement of the ZDDP molecule to form the LI-ZDDP isomer through the reaction of two dialkyldithiophosphate (DDP) anions, which may or may not be coordinated to the same zinc atom. Olefin formation then occurs through β-hydrogen transfer, and thiols are released as a result of nucleophilic attack at the phosphorus atoms. These processes leave a variety of (thio)-phosphate species that undergo a series of nucleophilic attacks at the phosphorus atom to result in the formation of trialkyl-tetrathiophosphates and a polyphosphate species that undergoes polymerization to form the antiwear film. The nucleophile involved in these processes was not specified and could be a DDP anion or another species present in the oil.

More recently, the solution decomposition of ZDDPs to result in thermal films on oxide surfaces has been examined with particular emphasis placed on the composition of the resulting wear pad.[18,28] Analysis showed that the antiwear pad existed in layers with long-chained polyphosphates at the surface of the film and short-chained polyphosphates in the bulk. The mechanism proposed to account for this layered structure involves the initial accumulation of ZDDP at the surface followed by thermooxidative decomposition due to interactions with oxidizing agents present in the oil, such as peroxides, or with the oxide surface that resulted in the formation of long-chained polyphosphates that were subsequently converted into short-chained species through further oxidation reactions with the oxide surface. The LI-ZDDP species was also implicated as an intermediate in the initial stages of this process.

Reaction conditions likely play a critical role in the formation of antiwear films, and it is these same conditions that make obtaining reliable and consistent data difficult, impairing the formulation of a complete mechanism to describe film formation. Indeed, several degradation pathways that exhibit a dependence on parameters such as temperature[37−39] and the presence of certain chemical species in oil[17,30,31,40,41] have been proposed in addition to those mentioned above, and it is likely that several competing processes of ZDDP film formation exist. Computational modeling provides a means to examine chemical species and reactions under specified conditions. Although the simulation conditions may not exactly correspond to those found in an engine, modeling allows for one to study the effect of parameters such as temperature and pressure as well as understand the influence of other chemical species on film formation at the atomic level.

Computational modeling has previously been used to obtain knowledge of the structural aspects of ZDDP molecules[42,43] and of the reactivity of specific atomic centers in ZDDP with O^{2-} ions,[44] which were used as a model for an iron oxide surface. The interaction of DDP anions, derived from ZDDPs, with iron oxide surfaces has also been examined as a possible model for the antiwear film, and a correlation between the binding energy of the ion on the iron oxide surface and the effectiveness of the antiwear films produced from ZDDPs with a variety of substituents was proposed.[45] Further computational studies employed this correlation to examine the effectiveness of several proposed ZDDP alternatives.[46] In these studies the mechanism of film formation was either assumed and only the expected products of the assumed mechanism were examined or the possible sites of initial interaction with a model for an oxide surface were proposed without any investigation of the subsequent steps leading to film formation. It would be beneficial, however, to examine the behavior of ZDDP molecules under a wide range of scenarios that can mimic possible engine conditions. Through such a study it would be possible to acquire atomic level information regarding the key steps of ZDDP film formation as well as the dependence on the engine environment. The first step into an investigation of this type is to examine the structure and behavior of isolated gas-phase ZDDP molecules at 0 K and at finite temperatures. This will provide a basis for further studies of the effects of various parameters on film formation and allow for a comparison of observed atomic-level properties to be made.

In the current study the results of such an initial investigation into the thermal decomposition of ZDDP additives are presented. Ab initio molecular dynamics (MD) simulations have been performed on a series of isolated gas-phase ZDDP monomers, dimers, and isomers with a wide variety of substituents to study the finite temperature behavior of these molecules. Static quantum chemical calculations at the density functional level of theory have also been performed to provide further insight into the results of the ab initio MD calculations, and to provide basic structural information about the ZDDP molecules. The particular substituents considered in this study are hydrogen (H), methyl (Me), ethyl (Et), isopropyl (^{i}Pr), *tert*-butyl (^{t}Bu), and phenyl (Ph) groups. These encompass a wide range of substituent types, and given evidence that suggests that the ability of ZDDP films to inhibit wear is dependent upon the type of substituent present.[47−51] This series of substitution may provide insight into fundamental properties and differences of ZDDPs at the atomic level. Thus, the goal of the current study is to examine the behavior of ZDDPs at finite temperature and, with the aid of static quantum chemical calculations, identify and characterize the key chemical species and reactions that occur as part of the thermal decomposition of ZDDPs. In brief, the remainder of this paper is as follows: the computational details are given in section II, the discussion follows in section III with a detailed discussion of the results of the simulations, and the conclusions are presented in section IV.

II. Computational Methods

Kohn−Sham density functional theory (DFT)[52,53] calculations used to determine the energies and molecular geometries of all species considered in this study were performed with the ADF2002.01 quantum chemistry package.[54−56] The gradient corrected exchange and correlation functionals of Perdew, Burke, and Ernzerhof[57] with revised parametrization of the

exchange functional by Zhang and Yang,[58] the revPBE functional of ADF, were utilized in conjunction with the LDA parametrization of Vosko, Wilk, and Nusair (VWN)[59] for the calculation of both the energies and gradients. For all static DFT calculations the valence shells of all atoms were treated with a basis set of triple-ζ Slater-type orbitals augmented with polarization functions, the standard TZP basis set in the ADF package, with the exception of the calculation of the dimerization energies of the Ph- and ^{t}Bu-substituted species in which a basis set of double-ζ Slater-type orbitals plus polarization functions, the DZP basis set in ADF, was used on the hydrogen atoms, with all other atoms being treated with the TZP basis set. Inner shells were treated with the frozen core approximation.

Special care must be taken in order to obtain a global minimum when performing geometry optimizations of the dimers since several unique conformations of the alkyl substituents on these molecules may exist. To accomplish this, a 1.0 ns molecular dynamics simulation was performed at 1000 K using the Dreiding force field[60] with Cerius^2.[61] One hundred structures were selected at regular intervals throughout this simulation, and the geometries of these structures were optimized with Gaussian98[62] at the PM3 level of theory.[63,64] The 10 unique lowest energy structures from these optimizations were then optimized within ADF as described in the preceding paragraph. Although a global minimum is not guaranteed by this procedure, it does allow for the systematic determination of a minimum energy structure from a large number of initial geometries.

To investigate the finite temperature behavior of the ZDDP molecules, Car-Parrinello ab initio MD[65] simulations were performed with the CPMD package, version 3.5.[66] Analytic pseudopotentials of Goedecker et al.[67,68] were used to treat all core electrons, and the valence electrons were explicitly treated with a basis set of plane waves with a cutoff of 70 Ry. Although the revPBE functional used in the ADF calculations described in the preceding paragraph has been shown to provide accurate energies for molecular systems,[69,70] this functional is not available in the CPMD package, and the gradient corrected exchange−correlation functional of Perdew, Burke and Ernzerhof,[57] referred to as the PBE functional, was used instead. The PBE functional is quite similar to the revPBE one.

A time step of 6.0 au, equal to 0.147 fs, was employed in all CPMD calculations which maintained energy conservation within $\pm$0.000 06 au with an oscillation period of $\sim$0.15 ps. Periodic boundary conditions were employed with a "super cell" technique in all CPMD simulations, and a minimum vacuum distance of 7 Å was maintained between periodic images to minimize spurious interactions between these images. Different simulation parameters, such as temperature and total simulation time, were used when studying the different ZDDP species, and the specific details of the simulations will be given when appropriate in the discussion.

III. Results and Discussion

The discussion of the results is separated according to the different types of ZDDP molecules considered in this study. The results of the calculations on the dimeric form are presented first since evidence exists that suggests that the ZDDP species may exist as a dimer or even higher order oligomer and hence it is important to explore the possibility that the dimer may be a more appropriate model for these calculations. An in-depth examination of the simulations of the monomeric form of the ZDDP additives follows in section b with particular emphasis placed on the results of the ab initio MD simulations which provide useful insight into the finite temperature behavior of these molecules. The LI-ZDDP isomer is then briefly considered in section c.

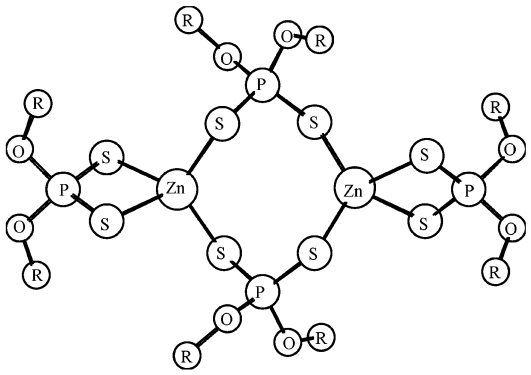

Figure 2. General structure of the ZDDP dimer. The label "R" refers to the substituent present on the ZDDP dimer.

a. ZDDP Dimers. It is well established that ZDDP molecules can exist in solution not only as monomers but also as dimers or even higher order oligomers.[71−73] The general formula of the ZDDP dimer is $Zn_2[PS_2(OR)_2]_4$, and based on information obtained through X-ray crystallography,[74,75] as well as through previous computational investigations,[42,43] it is known that the zinc atoms are connected by two bridging DDP groups and that each zinc atom is also chelated by one DDP group. This structure is shown in Figure 2.

Although virtually all mechanisms developed to explain the thermal decomposition of ZDDP molecules deal exclusively with the monomeric form,[28,29,34−38,40,41] it is possible that the dimer is a more realistic model with which to examine the behavior of ZDDP molecules. Previous studies have explored the relative stabilities of the H- and Me-substituted dimers, and the results indicated that the dimer is indeed a more stable species at 0 K.[42,43] At higher temperatures this may not be true, and thus it is of interest to explore the dynamics of the dimers at finite temperature and to calculate the dimerization energies of the ZDDP additives in order to aid in the development of an appropriate model upon which to perform further calculations. The results of finite temperature ab initio MD simulations of the H- and Me-substituted dimers are presented in part a(i). The calculated dimerization energies of all types of ZDDPs considered in this study are presented and discussed in part a(ii).

a(i). Molecular Dynamics Simulations. ZDDP antiwear films are formed under conditions that are typically found within running automobile engines where temperatures can easily reach 500 K.[10] To examine the likelihood of dissociation at finite temperature, ab initio molecular dynamics simulations were performed on the hydrogen- and methyl-substituted dimers at temperatures of 500 and 1000 K, which were held within $\pm$100 K by rescaling the atomic velocities, for 4.35 ps (30 000 time steps) each. Additionally, simulations in which an annealing scheme, through which the temperature was increased from an initial value of 300 K by scaling the atomic velocities by a factor of 1.000 25 at each time step, was employed to slowly increase the temperature of the system were also performed. The annealing scheme was used to minimize the possibility that any observed dissociations were artifacts of the random initial velocities that were assigned at the higher temperatures in the MD simulations. While the use of a thermostat may be desirable at these temperatures, particularly if quantitative information is to be obtained, such thermostats require long equilibration periods that would have made these calculations unfeasible. Since the purpose of the MD simulations was only to obtain

TABLE 1: Dimerization Energies for ZDDP Dimers

R[a]	ΔE(revPBE)[b]
H	−4.3
Me	2
Et	9.2
^{i}Pr	14.5
^{t}Bu	22.3
Ph	24.7

[a] R refers to the substituent on the ZDDP molecule. [b] ΔE(revPBE) = E_{dimer}(revPBE) − 2[$E_{monomer}$(revPBE)] in kcal/mol.

qualitative information about the chemical behavior of ZDDPs, little benefit would have been derived from the use of such thermostats, and it was decided that the use of the heating schemes outlined above would be sufficient. The results of the ab initio MD simulations revealed that at the lower temperature (500 K) the dimers exhibit very little interesting behavior on the time scale considered aside from the occasional dissociation of one of the bridging Zn−S bonds for a short period of time. At the higher temperature (1000 K) both the hydrogen- and methyl-substituted dimers readily underwent dissociation. It was observed that one of the Zn−S bonds underwent permanent dissociation at a temperature of ∼800 K when the annealing scheme was employed with a second bond dissociating at ∼1100 K to yield two separate ZDDP monomers. Analogous results were obtained through the simulation of the methyl-substituted dimer. It is stressed that the temperatures at which the bonds are reported to dissociate are not meant to be quantitative, but instead the results should be interpreted as demonstrating that the main process that the dimers undergo at finite temperature is dissociation to form the monomer. Furthermore, it is important to note that the results of the simulations did not show any unexpected behavior of this molecule at elevated temperature. That is, the molecule simply underwent dissociation to yield two monomers as one would expect, and hence the monomer may be a reasonable model for the study of the ZDDP additive at finite temperature. Ab initio MD simulations were not performed on the ethyl-, isopropyl-, *tert*-butyl-, and phenyl-substituted dimers since the simulations of the H- and Me-substituted dimers indicated that dissociation of this species readily occurs and it is unlikely that performing further simulations on these other species would provide any new information.

a(ii). Relative Energies. The results of the MD simulations indicated that the ZDDP dimer readily undergoes dissociation at elevated temperature. The dimerization energies for the ZDDP molecules with all of the substituents considered in this study have been calculated at the revPBE level of theory to further explore the likelihood of dissociation. This will allow for a quantitative examination of the favorability of the dissociation of the ZDDP dimer and will allow for the further assessment of the ZDDP monomer as a model upon which to perform further calculations. The calculated dimerization energies are given in Table 1. These results indicate that only the hydrogen-substituted dimer is stable with regard to dissociation (a negative dimerization energy indicates that the dimer is more stable). Previous studies[42] of the H-substituted dimer at the MNDO level of theory reported a dimerization energy of −7.8 kcal/mol for this species with the value calculated in the current study in relatively good agreement at −4.3 kcal/mol.[76] A dimerization energy of −5.6 kcal/mol has been reported in a previous Hartree−Fock study[43] of the methyl-substituted species; however, the current results indicate that the dimer is unstable by 2.0 kcal/mol with respect to the separated monomers. No dimerization energies, at the ab initio or semiempirical levels of theory, were available for comparison with the other substituted dimers.

The results of these calculations show that, in general, the relative energy of the dimer with respect to the monomer decreases as the bulk of the substituents increases. Thus it is likely that for the types of ZDDPs commonly used in motor oils, where substituents are typically large, the monomeric form is favored.[77] When temperature is applied, entropic contributions to the free energy will further favor the existence of the monomer. As a result of these findings, we determine that the monomeric form of ZDDP is a reasonable model upon which to perform the remainder of the calculations in this study.

b. ZDDP Monomers. Static DFT calculations and ab initio MD simulations were performed to identify key structures and decomposition products of the ZDDP monomer since it has been demonstrated that this form of the molecule is a suitable model for further study. The structures and energetics of the ZDDP monomers calculated with DFT are discussed in section b(i). Ab initio MD simulations were performed to explore the finite temperature dynamics of these molecules, and several interesting results were obtained. These results are presented individually to allow for their detailed examination.

The loss of coordination around the zinc atom at elevated temperature was observed during the MD simulations and is discussed in section b(ii). The dissociation of the ZDDP monomer to result in radical species was also observed and is discussed in section b(iii). Finally, elimination reactions leading to the loss of olefins and sulfides were observed and are discussed in section b(iv). Within sections b(ii) and b(iii) the results of the MD simulations are augmented with those of static DFT calculations to provide a further understanding of the observed behavior. These simulations shed light on atomic level differences in the behavior of different types of ZDDP molecules that may provide an explanation for certain observed macroscopic properties. The observation of this behavior through static quantum chemical calculations alone would not be possible.

b(i). Structures and Energies. Geometry optimizations of the ZDDP monomers were performed at the revPBE level of theory in order to determine the most stable form of these compounds. The structural aspects of the monomers are of significant interest in the study of ZDDPs and have been the focus of several previous theoretical and experimental investigations.[42,43,78,79] The bonding arrangement around the zinc atom is not well understood, particularly concerning whether the four Zn−S bonds are equivalent or if each of the DDP anions is coordinated to the central zinc atom through only one Zn−S bond with the other sulfur atom being doubly bonded to the phosphorus atom. Although these differences may seem slight, they are worth investigating in light of the fact that the zinc atom has indeed been identified as the preferential site for attack by O^{2-} anions[44] and nitrogen donor molecules[80] and that changes in the bonding around this atom may have an effect on its reactivity with nucleophiles.

The optimized geometries and relative energetics of ZDDP monomers with the alkoxy groups in a variety of configurations have been calculated. The conformations examined are equivalent to those identified as important minima on the potential surface for the Me-substituted ZDDP monomer in a previous investigation,[43] and we have adopted the naming convention used in that study. This naming convention is described in Figure 3. The relative energetics for each of the monomers are given in Table 2 along with structural data pertaining to the molecule with the alkoxy groups in the *tt* + *tt* conformation. Only structural data about this conformation is given since the

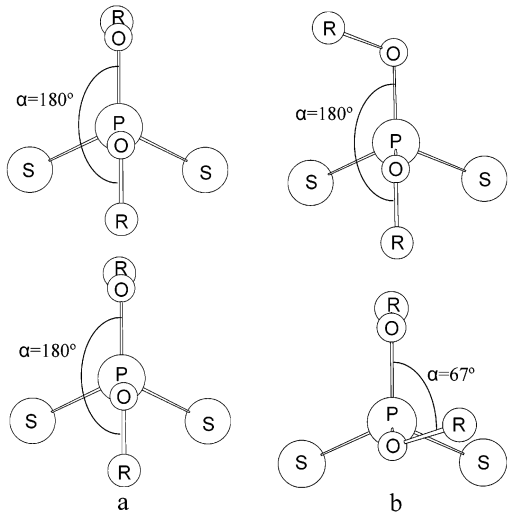

Figure 3. Conformations of alkoxy groups within a DDP group. Parts a and b show the *tt* and *tg* DDP groups from the perspective of each of the R substituents within a given DDP group. The angle α refers to the R−O−P−O dihedral angle. A *tt* conformation occurs when both dihedral angles, α, within a DDP group are equal to 180° as shown in (a), and a *tg* conformation refers to the situation when one angle is 180° and the other is ±67° as shown in (b). Thus in the ZDDP molecules, which contain two DDP groups, it is possible to have *tt* + *tt*, *tt* + *tg*, and *tg* + *tg* arrangements.

molecule exhibited very little variation in the geometry with changes in the orientation of the alkoxy groups and, in all cases, except for the ^{t}Bu-substituted monomer, this conformation was the most stable. Only *tt* and *tg* conformations of the alkoxy groups on each of the DDP groups were considered since these orientations have been shown to minimize interactions between alkyl groups.[43] A *gg* conformation is also possible but results in high energy interactions between R groups. High energy interactions also result with large substituents in the case that both values of α are equal to 0, and hence this conformation was not explored.

The data in Table 2 show slight variations in the relative energies of the ZDDP monomers with changes in the orientation of the alkoxy groups. In all cases, except with *tert*-butyl substituents, the monomer with the alkoxy groups in a *tt* + *tt* conformation is the most stable due to the minimization of high energy interactions between substituents (this conformer is more stable than the *tt* + *tg* one by 0.03 kcal/mol for both the ethyl- and isopropyl-substituted species). In all cases the *tg* + *tg* conformation is the highest energy structure, except when *tert*-butyl groups are present, where it is the most stable structure, due to the increase in high energy interactions between the alkyl substituents that result from this arrangement. These observations are in general agreement with the results of a previous study on the Me-substituted species.[43]

The optimized structures are in qualitative agreement with those reported in previous studies. It was found that all of the calculated structures exhibited a great deal of symmetry and that, in accordance with the results of previous calculations on these types of systems, the four Zn−S bonds are nearly equivalent, with the largest differences in these bond lengths within any of the ZDDP monomers being less than 0.01 Å. On a quantitative level the optimized structures exhibit some differences when compared with previously reported structures. Specifically, the bond lengths of the hydrogen-substituted monomer are all longer by 0.03−0.10 Å than in structures optimized at the MNDO level of theory[42] and the angles all exhibit differences larger than 5°, with the largest difference being ∼9° for the S−P−S angle. These differences likely result from the different levels of theory used to optimize the structures in the previous investigation and in the current one. The structure of the optimized methyl-substituted monomer agrees well with previously reported structures[43] with all bond lengths agreeing within 0.03 Å and all angles within 5°. No structures were available for comparison with the monomers with other substituents. It is interesting to note that the main structure of the ZDDP monomer (i.e., the structure not including the substituents) is rather insensitive to the type of alkyl group present. These results, as well as those reported in previous studies,[42,43] correspond to the structure in the zero temperature limit; however, since elevated temperatures are found in the engine environment, it is more important to examine the structure of the ZDDP monomer at higher temperatures.

b(ii). Loss of Coordination at the Zn Atom. Molecular dynamics simulations of the ZDDP monomers with all of the substituents considered in this study were performed at temperatures of both 700 and 1500 K. The temperatures were maintained within ±100 K of the target temperature (either 700 or 1500 K) by rescaling the atomic velocities for an initial period of 1.45 ps (10 000 MD time steps), after which the temperature constraints were removed and the simulation was allowed to continue for an additional 7.25 ps (50 000 MD time steps) for the H- and Me-substituted monomers and 2.90 ps (20 000 MD time steps) for the other ZDDP monomers. The lower of these two temperatures (700 K) was employed due to existing data that suggests that surface temperatures in engine tests commonly attain values of ∼500 K[10] and thus a temperature of 700 K is reasonably close while providing a slight increase in the kinetic energy of the system that may facilitate the observation of chemical behavior on the time scales considered in the simulations. A temperature of 1500 K is rather high in comparison to normal engine temperatures; however, it is likely that significantly higher than average temperatures may exist in very small regions of the oil and engine surface. It has also been proposed that surfaces in four ball machines used to study film formation commonly attain temperatures of 1000 K,[37] and thus the simulations at the higher temperature will allow for a comparison with experimental results. Performing the simulations at the higher temperature will increase the rate at which chemical processes occur; however, it must be noted that the higher temperature simulations will also favor dissociation processes.

The most prevalent behavior exhibited by the ZDDP monomers throughout the MD simulations was the dissociation of either one or two of the Zn−S bonds to form a complex in which the zinc atom is coordinated by three or two sulfur atoms, respectively. This change in the bonding arrangement was seen for all types of ZDDPs considered here and was observed at both simulation temperatures. The geometries of the species observed through the MD simulations contrast with those discussed in section b(i), where it was reported that all of the Zn−S bonds were equivalent. The bonding arrangement within the structures observed through the MD simulations are akin to those proposed in previous studies in which the DDP anion is coordinated to the zinc atom through one Zn−S bond with the remaining sulfur atom being doubly bonded to the phosphorus atom. The fact that this type of bonding is only seen at elevated temperature may shed light on the discrepancies in reported structures of the ZDDP monomer since at higher temperature it is possible for the molecule to adopt a variety of forms.

A plot of the four Zn−S distances of the hydrogen-substituted ZDDP monomer versus time at 700 K is given in Figure 4 and clearly shows several aspects of the bonding around the zinc

TABLE 2: Relative Energies[a] and Relevant Structural Data[b] of the ZDDP Monomers

			bonds (Å)			angles (deg)		
R[c]	conformation[d]	ΔE	Zn−S	P−S	P−O	Zn−S−P	S−P−S	O−P−O
H	*tt* + *tt*	0.0	2.445	2.031	1.634	80.6	111.8	93.3
	tt + *tg*	0.8						
	tg + *tg*	1.8						
Me	*tt* + *tt*	0.0	2.442	2.037	1.626	80.8	111.3	94.2
	tt + *tg*	0.5						
	tg + *tg*	0.9						
Et	*tt* + *tt*	0.0	2.438	2.039	1.625	80.9	110	95.4
	tt + *tg*	0.0						
	tg + *tg*	0.5						
^{i}Pr	*tt* + *tt*	0.0	2.436	2.046	1.621	81.4	110.1	94.9
	tt + *tg*	0.0						
	tg + *tg*	3.0						
^{t}Bu	*tt* + *tt*	0.0	2.433	2.049	1.618	81.1	110.2	93.5
	tt + *tg*	−0.5						
	tg + *tg*	−0.9						
Ph	*tt* + *tt*	0.0	2.448	2.023	1.646	80.5	112.1	91.7
	tt + *tg*	0.9						
	tg + *tg*	1.2						

[a] Energies are in kcal/mol at the revPBE/TZP level of theory relative to the *tt* + *tt* conformer. [b] Only structural data for the *tt* + *tt* conformer are given. [c] R refers to the substituent on the monomer. [d] The conformation of the alkoxy groups is as described in Figure 3.

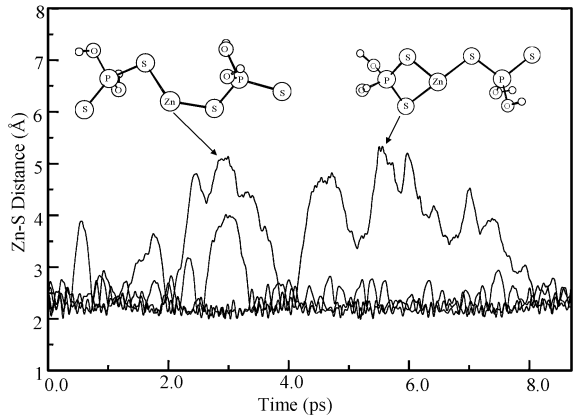

Figure 4. Lengths of the four Zn−S bonds versus time for the hydrogen-substituted ZDDP monomer at 700 K. The two chemical structures in the plot are snapshots taken from the MD simulation and show the bonding structure of the molecule at the two points indicated by the arrows.

atom at finite temperature. Throughout the duration of the simulation there are a minimum of two sulfur atoms coordinated to the central zinc atom as shown by the Zn−S bond lengths which oscillate around a value of approximately 2.3 Å; recall that this bond length in the optimized monomer was 2.445 Å. It was also observed that one of the Zn−S bonds dissociates early on in the simulation and remains dissociated for extended periods of time, periodically coordinating to the zinc atom. Occasionally a second Zn−S bond would dissociate, for example at ∼3.0 ps in Figure 4, with the resulting species being one in which the zinc was coordinated by two sulfur atoms, each of which belonged to different DDP ligands. Analogous data were obtained for the simulations of ZDDP monomers with other substituents. At the higher temperature the same behavior was observed with the dicoordinate structure persisting for longer periods of time.

It is important to note that in no case does the dissociation of the Zn−S bonds result in the formation of a free DDP anion, which has previously been proposed as a model for the decomposition products of ZDDP in solution and as a key intermediate in ZDDP film formation.[45,81,82] That is, for all substituents and temperatures considered the ZDDP molecule remained intact at the zinc atom with the coordination at that

TABLE 3: Energies of the Tri- and Dicoordinate ZDDP Monomers Relative to the Tetra-coordinate Monomer

	ΔE[a]	
R[b]	tricoordinate	dicoordinate
H	10.2	23.3
Me	11.5	23.9
Et	11.2	23.2
^{i}Pr	13.8	27.9
^{t}Bu	13.9	22.1
Ph	12.0	27.3

[a] The energies are in kcal/mol at the revPBE/TZP level of theory relative to the tetracoordinate monomer with the alkoxy groups in *tt* + *tt* conformation. [b] R refers to the substituent on the monomer.

atom changing to either 3 or 2. The energies of the optimized structures of the di- and tricoordinate species relative to those of the tetracoordinate ZDDP monomers are given in Table 3. These values indicate that the structures with decreased coordination at the zinc atom are unstable with respect to the tetracoordinate species, with the dissociation of one Zn−S bond leading to an increase in energy by ∼10−14 kcal/mol and the breaking of a second bond further increasing the energy by ∼9−16 kcal/mol; however, at finite temperature entropic contributions to the free energy will favor the dissociation of the Zn−S bonds. The results of these simulations thus indicate that at finite temperatures, particularly those consistent with running engine temperatures, the bonding around the zinc atom of the ZDDP monomer is such that four equivalent Zn−S bonds do not exist.

The dissociation of the Zn−S bonds decreases the steric hindrance at the zinc and hence may facilitate attack of this atom by nucleophiles. The loss of coordination at the zinc atom also has an effect on the electronic structure of the system, particularly by decreasing the energy of the lowest unoccupied molecular orbital (LUMO). The Kohn−Sham LUMO of the hydrogen-substituted ZDDP monomer is shown in Figure 5 as the number of Zn−S bonds decreases from four to two along with the energy of this orbital (ϵ_{LUMO}) in each case. It is apparent that the LUMO consists of atomic orbitals centered on the zinc atom participating in antibonding interactions with orbitals on the neighboring sulfur and phosphorus atoms. As the number of Zn−S bonds decreases, two clear observations regarding the LUMO are made. First, ϵ_{LUMO} decreases with the number of Zn−S bonds, and second, the LUMO becomes more localized

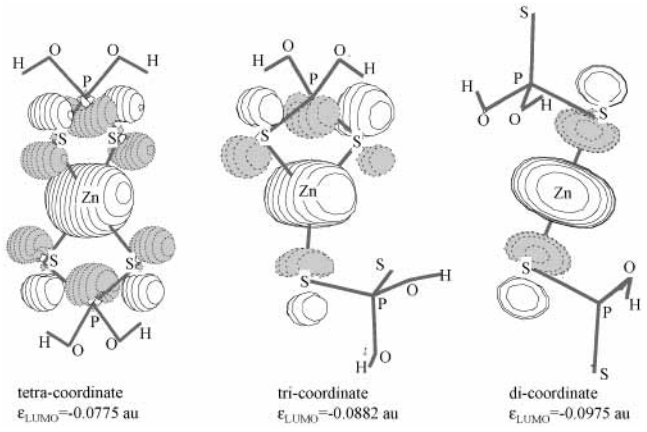

Figure 5. LUMO and ϵ_{LUMO} of the ZDDP monomer as the number of Zn−S bonds decreases from 4 to 3 to 2. The wave function is plotted at a value of 0.05 au.

on the zinc atom with the percent contribution of atomic orbitals on the zinc to this molecular orbital increasing from 43.4% to 65.3% as the number of Zn−S bonds changes from four to two. These two factors lead to an increase in the electron-accepting ability of the zinc atom, and hence the coordinatively unsaturated species will exhibit a greater reactivity with nucleophiles at the zinc atom. Analogous trends were obtained for the ZDDP monomers with other substituents. It is also noted that the LUMO has considerable contributions from the sulfur atoms that are coordinated to the zinc and that the steric hindrance at these atoms decreases as the coordination at the zinc decreases, which may also facilitate nucleophilic attack at the sulfur atoms.

This result has particular ramifications regarding mechanisms that postulate that the phosphorus atoms undergo nucleophilic attack during decomposition.[28,35,36] As the coordination at the zinc atom decreases, the total contribution of atomic orbitals on the phosphorus atoms to the LUMO decreases from 20.0% when four Zn−S bonds exist to less than 1% in the dicoordinate structure; thus the likelihood of nucleophilic attack at the phosphorus atoms is lowered. Examination of higher energy virtual orbitals showed that contributions from the phosphorus atoms first became significant for the LUMO+3 orbitals in the cases of the tetra-, tri-, and dicoordinate species, with this orbital being approximately 0.05 au higher in energy than the LUMO in each case. This indicates that attack at the phosphorus atoms is possible; however, it is a higher energy process than attack at the zinc and is thus less likely to occur. These conclusions are consistent with experimental[80] and theoretical[44] studies that indicate that nucleophilic attack preferentially occurs at the zinc atom. The investigation of ZDDP molecules with other chemical species will be the focus of a future investigation.

b(iii). Radical Elimination Reactions. The finite temperature simulations of the ZDDP monomers also revealed significant differences between the ZDDPs with aryl and alkyl substituents, particularly regarding the preferred types of dissociation reactions that these species take part in. Based on these simulations, two competing dissociation processes, outlined in Scheme 1, were identified involving the loss of either alkyl or alkoxy radicals. In general, it was observed that the loss of alkyl radicals was favored when aliphatic substituents were present on the ZDDP molecule. On the other hand, dissociation through the loss of alkoxy radicals occurred for the phenyl-substituted species. The observation of these processes will be examined first, and a discussion of the significance of these results will follow.

It was observed through the ab initio MD simulation of the *tert*-butyl-substituted species at 700 and 1500 K that a *tert*-butyl radical was ejected from the molecule shortly after the simulation started. This is demonstrated in Figure 6, where the distance of the C−O bond connecting the *tert*-butyl substituents that is lost as a radical to the remainder of the ZDDP molecule is plotted along with the net spin density of the system against time for the first 1.0 ps of the MD simulation at 1500 K. The net spin density shown in this plot is that obtained by integrating both spins over all space and does not correspond to the eigenvalue of the spin operator. The plot shows that at a time of ∼0.2 ps the C−O bond begins to dissociate. A sharp increase in the net spin density of the system to a value corresponding to ∼2 unpaired electrons also occurs at this time and is consistent with the loss of one of the alkyl groups as a radical species. The reason that the increase in the net spin density occurs slightly after the bond dissociates is due to the system maintaining a closed-shell electronic structure before making a sudden jump to an open-shell one. The alkyl radical loss leaves a lone electron on one of the oxygen atoms, which is a potential site for the formation of linkages between phosphate groups that could lead to polymerization yielding antiwear films. It was also observed that once elimination of the alkyl radicals occurred the dealkylated oxygen occasionally interacted with the zinc atom through the formation of Zn−O bonds. The loss of alkyl radicals was not observed in the simulations of any of the other ZDDP monomers considered in this study; however, this may be due to the decreased stability of the radicals formed through these processes in conjunction with the short time intervals examined in these simulations.

Similar results leading to the loss of two phenoxy radicals were observed through the 1500 K simulation of the phenyl-substituted ZDDP monomer. At a time of approximately 0.8 ps two of the P−O bonds within the phenyl-substituted monomer started to dissociate. This coincided with a sharp increase in the net spin density of the system to a value corresponding to between three and four unpaired electrons at a time of ∼0.9 ps, which was maintained throughout the remainder of the simulation (not shown). This result is consistent with the formation of two phenoxy radicals. None of the aliphatic-substituted ZDDP monomers showed any indication of cleavage at the P−O bond; hence this result demonstrates a significant difference in the atomic level behavior of the aliphatic- and aryl-substituted species at finite temperature.

The energetics of reactions a and b in Scheme 1 were calculated at the revPBE level of theory to determine the relative likelihoods of these two processes. The calculated energies for these processes are shown in Table 4. The data show that the loss of alkyl radicals is favored over the loss of alkoxy radicals for all substituents considered in this study except for phenyl groups, although both processes lead to an increase in the energy of the system. On the other hand, when examining the phenyl-substituted species, it is clear that the loss of a phenoxy radical is favored over the loss of a phenyl radical. This results from the stabilization of the phenoxy radical due to resonance effects that distribute the lone electron on the oxygen atom over the *o*- and *p*-carbon atoms of the phenyl ring. This type of resonance is not possible within the phenyl radical that would be formed through C−O bond dissociation in the phenyl-substituted ZDDP.

These results are no unexpected; however, the fact that there is a clear difference in the observed dissociation pathways of the alkyl- and aryl-substituted species is significant in light of the experimental evidence that shows that ZDDP antiwear films derived from aryl-substituted additives offer significantly less

SCHEME 1: Dissociation Processes Considered as a Result of Molecular Dynamics Simulations[a]

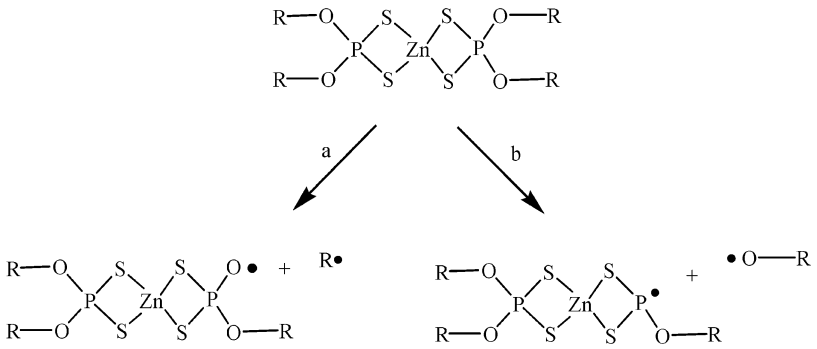

[a] Reaction a is the loss of alkyl radicals, and reaction b involves the loss of alkoxy radicals. The label "R" refers to the alkyl substituent on the ZDDP molecule.

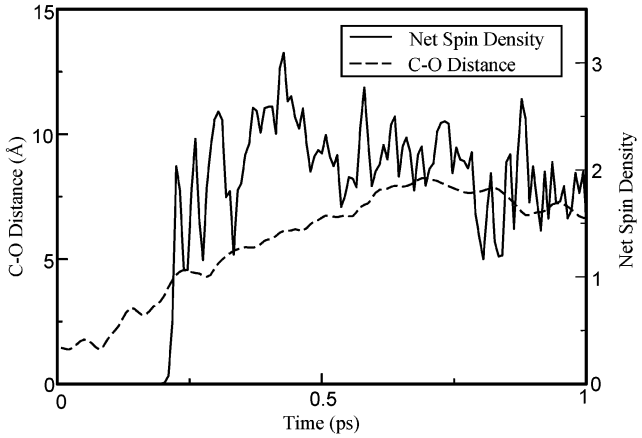

Figure 6. C−O bond distance of the *tert*-butyl group that underwent elimination as a radical along with the net spin density of the system versus time for the simulation of *tert*-butyl-substituted ZDDP at 1500 K.

TABLE 4: Energies[a] **for the Progression from Reactants to Products for the Processes Described in Scheme 1**

R[b]	*E*(a)[c]	*E*(b)[d]
H	88.1	103.5
Me	63.3	82.5
Et	64.6	81.2
^{i}Pr	61.7	81.1
^{t}Bu	55.5	76.1
Ph	72.2	59.0

[a] Energies are in kcal/mol at the revPBE/TZP level of theory. [b] R refers to the substituent on the ZDDP monomer. [c] *E*(a) corresponds to reaction a in Scheme 1. [d] *E*(b) corresponds to reaction b in Scheme 1.

antiwear protection than those derived from alkyl-substituted ZDDPs.[47−51] It has previously been proposed that the nature of the differences in the qualities of these films may lie in the differences in binding energies of the corresponding DDP anions with oxide surfaces;[45,46] however, the results of the current study indicate that the formation of these ions does not occur during the unimolecular dissociation of ZDDPs and hence the observed macroscopic differences are possibly of a different origin.

We provide an alternative explanation for the observed macroscopic differences based on the type of dissociation pathway that the ZDDP molecule follows. This explanation is based on the idea that ZDDP antiwear films consist of (thio)-phosphate chains and that the resiliency of the films to wear increases with the number of linkages between (thio)phosphate units. These units are connected by P−O−P (or P−S−P) linkages, and thus the presence of oxygen (or sulfur) is necessary to form these connections. Although both types of radical loss described above leave moeities containing the necessary elements to form the ZDDP films, the loss of alkoxy radicals removes oxygen from the system, which decreases the number of available sites for linking within the ZDDP antiwear film. As a result, the films formed from aryl-substituted ZDDPs, which were shown to preferentially undergo the loss of alkoxy radicals, are of poorer quality than those derived from alkyl-substituted ZDDPs which take part in radical dissociation processes that do not remove oxygen from the precursors to the antiwear film. It should be noted that this explanation is based on data obtained for the isolated ZDDP monomers. Under typical engine conditions oxygen-containing chemical species are present that may replace some of the oxygen lost due to alkoxy radical elimination.

b(iv). Olefin and H_2S Elimination. The loss of olefins was observed during the ab initio MD simulations of the *tert*-butyl-substituted monomer at both temperatures considered in this study. At the higher temperature the formation of hydrogen sulfide was also observed. The formation of these species is known to occur throughout the solution decomposition of ZDDP additives,[34] and hence these simulations may provide insight into the nature of the formation of these compounds. Additionally, these processes result in the formation of (thio)phosphate species that may be the precursors to the antiwear film.

Two distinct mechanisms for the elimination of olefins from the ZDDP monomer were observed through the ab initio MD simulations: the first involves the formation of a radical intermediate while the second is a concerted process. These two processes yield different products and are outlined in parts a and b, respectively, of Scheme 2. In the radical process an alkyl radical is formed through the dissociation of a C−O bond as described in section b(iii). This radical remains in close proximity to the remaining portion of the ZDDP molecule, and after a period of time, a hydrogen atom is abstracted from the radical by the dealkylated oxygen atom. This results in the formation of an O−H bond and the release of an alkene. The concerted elimination involves the transfer of a β-hydrogen from the alkyl group to an adjacent sulfur atom along with the simultaneous dissociation of a C−O bond to result in the formation of an alkene. Snapshots from the MD trajectories that outline this process are shown in Figure 7a−c for the *tert*-butyl-substituted ZDDP monomer. In Figure 7a the ZDDP molecule, minus one alkyl group that was previously lost as a radical, is in the tricoordinate form discussed in section b(ii) and the ^{t}Bu group approaches the sulfur atom to initiate the transfer of the hydrogen atom. The transfer of the β-hydrogen from the ^{t}Bu group to the sulfur atom then takes place as shown in Figure

SCHEME 2: Mechanisms for Elimination of Olefins and Sulfides from the *tert*-Butyl ZDDP Monomer[a]

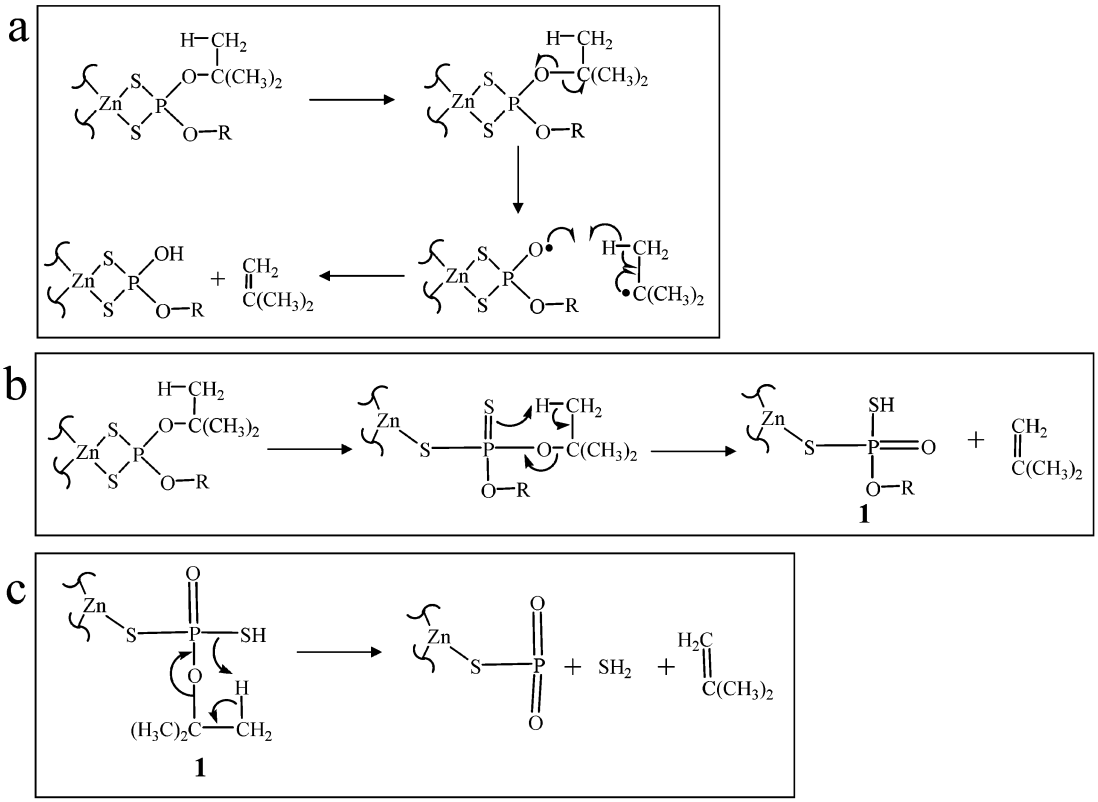

[a] Reaction a corresponds to the elimination of an olefin through an alkyl radical intermediate, reaction b depicts the concerted loss of an olefin, and reaction c, which starts from the product of reaction b labeled **1**, shows how sulfide elimination occurs along with the olefin elimination. Only half of the ZDDP molecule is shown to reduce the size of the structures.

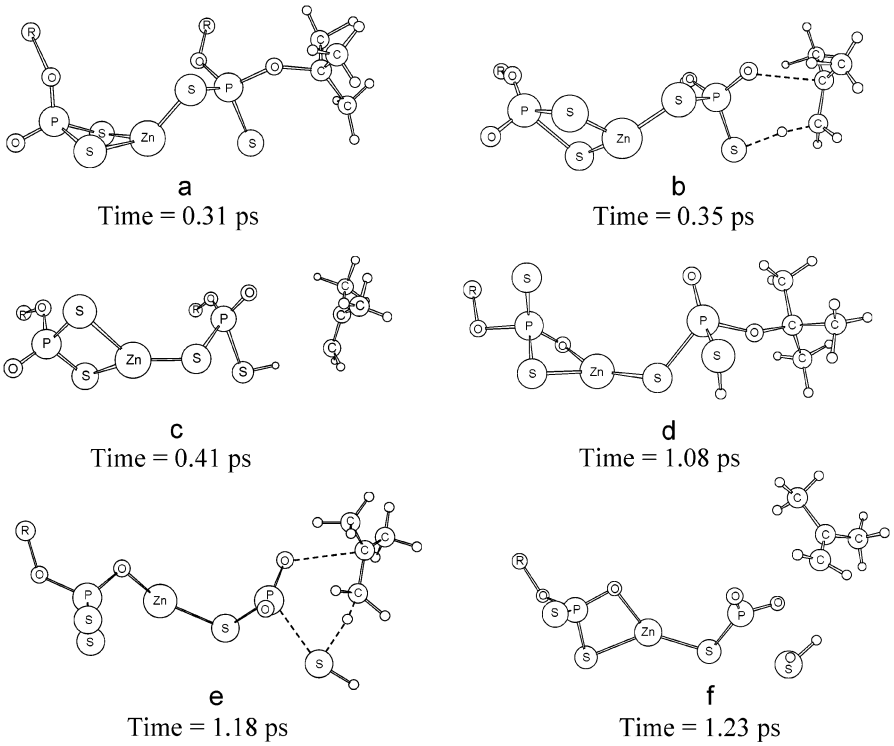

Figure 7. Snapshots from MD simulations outlining the sulfide elimination process from *tert*-butyl-substituted ZDDP monomer. Note that some of the alkyl groups have been replaced by a general "R" symbol for clarity within the figure. Also note that one of the alkyl groups is missing from the ZDDP. This lost group corresponds to a ^{t}Bu group that was lost as a radical as described in section b(iii). The processes depicted in this figure are described in the text.

7b, and the olefin is then released as depicted in Figure 7c. This mechanism is analogous to that previously proposed to account for olefin elimination.[34] However, in that study it was indicated that the olefins were derived from the LI-ZDDP isomer

and that the β-hydrogen transfer occurred between the alkyl group and an oxygen atom, rather than a sulfur atom.

The products formed through the radical and concerted processes are quite similar, with the main difference being the formation of either O−H or S−H bonds for the radical and concerted processes, respectively. It is interesting to note that it is possible to generate the hydrogen-substituted monomer through the elimination of all four olefins through a radical intermediate. Similarly, the hydrogen-substituted LI-ZDDP isomer, with four hydrogens transferred from the oxygens to the sulfurs, could be formed through the loss of all four alkyl groups through the concerted mechanism. Intermediate degrees of isomerization toward the LI-ZDDP isomer could also be formed if both processes occurred within the ZDDP monomer.

It was also observed that the formation of H_2S was possible as a side reaction of the olefin elimination. The formation of H_2S is known to occur throughout the thermal decomposition of ZDDP molecules.[34] The results of the MD simulations showed that H_2S molecules were formed if two olefin eliminations occurred within the same ZDDP molecule through the concerted process described above. In that mechanism a hydrogen was transferred from the alkyl group to a sulfur atom. If two such transfers occur to the same sulfur atom, it is possible for a molecule of H_2S to be formed.

This process is outlined in Scheme 2c and by the snapshots taken from the MD trajectories of the *tert*-butyl-substituted ZDDP monomer at 1500 K that are shown in Figure 7d−f. In Figure 7d the portion of the ZDDP molecule remaining after the first olefin elimination is shown and one of the alkyl groups previously designated with an "R" has been replaced with a ^{t}Bu group. In Figure 7d a Zn−O bond has also formed due to the interaction of a dealkylated oxygen with the zinc atom. In Figure 7e a second transfer of a β-hydrogen from the ^{t}Bu group to the sulfur atom occurs. Finally, in Figure 7f the formation of the olefin and H_2S is complete. It is apparent that since the elimination of two olefins, separated by an interval in time, and subsequent loss of H_2S was observed to occur through the simulation of the *tert*-butyl-substituted ZDDP monomer at 1500 K within the short period of time (4.35 ps) considered in the simulation, both of these elimination reactions are facile processes.

The observation of these two reactions further highlights differences between alkyl- and aryl-substituted ZDDPs that may have ramifications on the antiwear properties of the resulting film. The loss of olefins leaves behind a chemical species containing all of the elements necessary to form the (thio)-phosphate units that are thought to be the building blocks of the antiwear films. It was observed, however, that the loss of the olefins to form these species occurred through the transfer of a β-hydrogen from the alkyl group to the remainder of the ZDDP molecule. Thus, this process should occur at a faster rate for alkyl groups that contain a greater number of β-hydrogens or for groups that contain more acidic hydrogens. This is consistent with the observations that films derived from ZDDPs with secondary alkyl groups are formed faster than those with primary alkyl or methyl substituents (in practice tertiary alkyl substituents are not used).[17,18,28] The transfer of a β-hydrogen from the phenyl group would result in the formation of benzyne, which is a highly unstable species. As a result, it is unlikely that this hydrogen transfer would occur, which may lead to a decrease in the rate of film formation and contribute to the decreased antiwear ability of films formed from aryl-substituted ZDDPs.

It was noted above that in the ZDDP films the (thio)phosphate units are linked through P−O−P or P−S−P bonds. The elimination of sulfides from the molecule will reduce the sulfur content and thus decrease the possibility of forming such linkages. However, in a typical engine a variety of chemical species are present, such as peroxides and water, which can provide oxygen to replace the lost sulfur groups. If this replacement occurs quickly enough, more P−O−P linkages will form within the (thio)phosphate polymer, as opposed to P−S−P linkages, which will improve the antiwear effectiveness of the resulting film. The sulfide elimination is unlikely to occur for the aryl-substituted ZDDPs through the mechanism observed in this study, since olefin elimination through the concerted mechanism is improbable, and thus the replacement of P−S−P bonds is less likely to take place. This may also contribute to the poorer antiwear performance of films derived from aryl-substituted ZDDPs.

c. LI-ZDDP Isomers. The LI-ZDDP isomer has been implicated as an important species in the decomposition of ZDDP additives to form antiwear films.[18,28,34−36] The structures and energies of the LI-ZDDP species, relative to those of the normal ZDDP monomer, are presented in section c(i). Ab initio MD simulations of the isomers were also performed and have shown that at finite temperature the LI-ZDDP isomer behaves quite similarly to the normal ZDDP monomer. It was observed that the coordination at the zinc atom fluctuated throughout the simulation for all the substituents considered. The ^{i}Pr- and ^{t}Bu-substituted isomers underwent olefin elimination and alkyl radical loss, respectively, while the Ph-substituted species exhibited alkoxy radical elimination at finite temperature. Since these processes have already been discussed in detail, they will only briefly be covered here in order to reduce redundancy within the discussion. The results of the ab initio MD simulations are discussed in section c(ii). To the best of our knowledge this is the first example of a study of this isomer by theoretical means.

c(i). Structures and Energies. The LI-ZDDP isomer is formed through the transfer of one or more alkyl groups from the oxygen atoms to the sulfur atoms of the ZDDP. Since four alkyl groups are present on the ZDDP molecule, four transfers of these groups are possible and thus varying degrees of isomerization can exist. In the current study the isomer resulting from the transfer of only one alkyl group, as shown in Figure 1b, has been examined as a model. It should be noted, however, that mechanisms for the thermal decomposition of ZDDP have been proposed that involve varying degrees of isomerization;[18,28,35,36] the study of these types of LI-ZDDP isomers will be the focus of future study.

The energies of the optimized LI-ZDDP isomers are shown in Table 5 along with relevant structural data around the zinc atom. Only the structural data around this atom is given since the geometry of the rest of the molecule was relatively unaffected by the isomerization when compared with the normal tetracoordinate ZDDP monomer. The energies of the isomer, relative to the most stable conformation of the normal ZDDP monomer for each of the different types of substituents considered in this study, indicate that the LI-ZDDP isomer is similar in energy with the normal ZDDP monomer. This is an interesting result since the relative populations of the ZDDP and LI-ZDDP species in oil will be thermodynamically controlled and hence these two species may exist in relatively similar quantities in the engine. Furthermore, an increase in the reactivity of the LI-ZDDP species is implied by the proposed mechanisms that indicate that the isomerization is a necessary

TABLE 5: Energies of the LI-ZDDP Isomers Relative to the Energies of the Corresponding Normal ZDDP Monomer

		bonds (Å)				angles (deg)
R[a]	ΔE[b]	Zn−O	Zn−S[c]	Zn−S	Zn−S	P−Zn−P
H	5.4	2.160	2.435	2.480	2.426	159.7
Me	−5.0	2.136	2.408	2.436	2.439	168.6
Et	−2.0	2.144	2.401	2.398	2.470	157.3
^{i}Pr	2.6	2.155	2.396	2.404	2.459	157.3
^{t}Bu	0.5	2.166	2.389	2.397	2.459	157.2
Ph	0.4	2.140	2.403	2.404	2.455	159.7

[a] R refers to the substituent on the LI-ZDDP molecule. [b] ΔE is the energy of the LI-ZDDP isomer relative to the most stable corresponding ZDDP monomer in kcal/mol at the revPBE/TZP level of theory. [c] This is the Zn−S bond from the same DTP group that has the Zn−O bond.

step in the formation of ZDDP antiwear films; however, these results indicate that this is not due to the instability of the LI-ZDDP isomer relative to the normal ZDDP monomer.

Based on the structural data given in Table 5, it is apparent that the bonding around the zinc atom is no longer equivalent. This change in the bonding arrangement is due to the Zn−O distance being significantly shorter than the three Zn−S bond lengths. This disrupts the symmetry around the zinc atom that was exhibited in the normal ZDDP monomer and leads to a decrease in the P−Zn−P angle from ∼180°, as was exhibited in the normal monomer, by several degrees. However, the Zn−O bond length is longer than the typical Zn−O bond distance of 1.988 Å for the wurzite structure of ZnO,[83] and this decreases the interaction of the oxygen atom with the zinc atom. As a result of the distortion in the geometry around the zinc atom, the Zn−S bond lengths of the DDP group with two Zn−S bonds are also no longer equivalent, except in the case of the Me-substituted isomer, with one Zn−S bond being significantly shorter than the other. The Zn−S bond of the other DDP group also exhibits a decrease in length when compared to the normal ZDDP monomer that likely occurs to compensate for the decreased coordination at the zinc atom by the oxygen atom.

c(ii). Finite Temperature Behavior. As mentioned above, it was observed that the finite temperature behavior of the LI-ZDDP isomer was quite similar to that of the normal ZDDP monomer. Once again, ab initio MD simulations were performed at temperatures of 700 and 1500 K. For all of the substituents considered in this study, these temperatures were held within ±100 K for an initial period of 1.45 ps (10 000 MD time steps) followed by a further 7.25 ps (50 000 MD time steps) of simulation for the H- and Me-substituted isomer and a further 2.90 ps (20 000 MD time steps) of simulation for all of the other isomers. The reasons for the selection of these particular temperatures are discussed in section b(ii).

The results of the MD simulations showed that the coordination at the zinc atom fluctuated with time. It was observed that at no point did the dissociation of the Zn−S, or Zn−O, bonds result in the formation of a free DDP anion and that within the tri- and dicoordinate structure the zinc could be coordinated by either the sulfur atoms or the oxygen atom. Throughout the 1500 K simulation of the *tert*-butyl-substituted LI-ZDDP isomer the elimination of two alkyl radicals was observed. One ^{t}Bu radical was lost from each side of the LI-ZDDP isomer; that is, elimination occurred from both the DDP group that is identical to those in the normal ZDDP monomer and from the rearranged DDP group. In both cases the radicals were formed through the dissociation of C−O bonds and not through the dissociation of the C−S bond. During the simulation of the ^{i}Pr-substituted species an increase in the net spin density of the system was observed to occur along with an elongation of one of the C−O bonds; however, this did not lead to the loss of a radical. Alkyl radical elimination was not observed for any of the LI-ZDDP isomers with other substituents. Alkoxy radical elimination was exclusively observed for the phenyl-substituted LI-ZDDP isomer. This is consistent with the results presented in section b(iii) that indicated that aryl-substituted ZDDPs undergo the loss of alkoxy radicals whereas alkyl radicals are eliminated from ZDDPs with aliphatic substituents.

Olefin elimination was observed only in the case of the isopropyl-substituted LI-ZDDP isomer at 1500 K and occurred through a process similar to the concerted mechanism for olefin elimination from the normal ZDDP monomer that was discussed in section b(iv). This process should also have been possible for the ^{t}Bu-substituted isomer; however, this was not observed perhaps due to the fact that two of the alkyl groups were readily lost as radicals. The fact that the olefin elimination was observed to occur with ^{i}Pr substituents may indicate that this process is easier within the LI-ZDDP isomer. The major difference between the elimination from the LI-ZDDP isomer and the ZDDP monomer was that for the LI-ZDDP the hydrogen was transferred from the alkyl group attached to the sulfur atom to the oxygen atom that was originally coordinated to the zinc atom, whereas for the normal ZDDP monomer the hydrogen was transferred to a sulfur atom. The observed concerted process for the elimination of olefins from the LI-ZDDP species is identical to that proposed in a previous experimental study of the thermal decomposition of ZDDPs in solution.[34] It is noted that the transfer of the hydrogen to one of the sulfur atoms originally coordinated to the zinc atom is also possible although it was not observed in these simulations. Furthermore, since one of the DDP groups in the LI-ZDDP molecule is identical to that in the ZDDP monomer and the two sides of the molecule act rather independently of one another since they are separated by a large distance, olefin elimination through either of the mechanisms discussed in section b(iv) should also be possible; however, they were not observed.

Thus, based on the results of the finite temperature MD simulations of the LI-ZDDP isomers, it is apparent that the behavior of this species is quite similar to that of the normal ZDDP monomers. Once again, olefin elimination was observed to yield (thio)phosphate species that may lead to the formation of antiwear films and the olefin elimination process involved the transfer of a β-hydrogen. This supports the argument developed in section b(iv), where it was proposed that the observed correlation between the number of β-hydrogens and the rate of film formation is due to this olefin elimination process. Differences between the behavior of LI-ZDDP species with aryl and alkyl substituents that were in agreement with those reported for the ZDDP monomers were also observed, particularly regarding the loss of radicals. Once again, these differences may have significant ramifications regarding the antiwear capabilities of films derived from these species.

Furthermore, the fact that similar types of antiwear film precursors can be formed through the thermal decompositions of the ZDDP monomer and the LI-ZDDP isomers indicates that the formation of the LI-ZDDP isomer is not absolutely necessary

in the formation of ZDDP thermal films; however, the isomerization will not hinder the formation of these films. In fact, the olefin elimination from the ^{i}Pr-substituted isomer indicates that some processes that may lead to antiwear film formation may be more facile for this species.

IV. Conclusions

The structures, energies, and finite temperature dynamics of ZDDP monomers, dimers, and isomers with a wide variety of substituents have been examined with static DFT calculations and through ab initio molecular dynamics simulation. The investigation of the structures of these species indicated that at finite temperature the ZDDP additives likely exist in the monomeric form. Furthermore, it was shown that at finite temperature this species undergoes facile dissociation of one or two of the Zn−S bonds and that this dissociation has an effect on the electron-accepting abilities of the monomer. An examination of the relative energetics of the monomer and its isomer, LI-ZDDP, revealed that these two species are of similar stability.

The finite temperature simulations of both the ZDDP monomer and LI-ZDDP isomer allowed for the identification of several distinct thermal decomposition pathways involving the loss of radicals, olefins, and sulfides. Alkyl-substituted ZDDPs underwent the preferential loss of alkyl radicals, whereas aryl-substituted species decomposed through the elimination of the alkoxy radicals. Both processes result in the formation of (thio)phosphate species that may be precursors to the antiwear film, but those resulting from the loss of alkoxy radicals have a decreased oxygen content and may result in the formation of a film of poor quality. This difference in the decomposition pathways highlights a difference between aryl and alkyl-substituted ZDDPs and may provide a possible atomic level explanation for experimental results that indicate that films generated from aryl-substituted ZDDPs offer significantly less antiwear protection than those derived from alkyl-substituted additives.

The loss of olefins was also observed to occur through either of two distinct mechanisms involving radical intermediates or concerted processes. Both of these elimination mechanisms involved the transfer of a β-hydrogen from the alkyl group and led to possible precursors to the antiwear films. Thus, for substituents that contain a greater number of these atoms, the formation of the antiwear film is more easily achieved, which is consistent with experimental observations. Furthermore, this process is not likely to occur for aryl-substituted ZDDPs and may further contribute to the reduced antiwear abilities of films derived from aryl-substituted additives.

Acknowledgment. We thank Dr. P. Norton from the University of Western Ontario and Dr. L. Hector, Jr., Dr. Yue Qi, Dr. Y-T. Cheng, and Dr. W. Capehart from General Motors Research and Development for many useful discussions. We gratefully acknowledge the Natural Sciences and Engineering Research Council of Canada (NSERC), General Motors Canada, and General Motors Research and Development for financial support. Computing resources made available by the Canada Foundation for Innovation, the Ontario Innovation Trust, SHARCnet of Canada, and the Academic Development Fund at the University of Western Ontario are also acknowledged.

Supporting Information Available: Cartesian coordinates and total energies of all optimized stationary points. AVI movie files of selected trajectories. This material is available free of charge via the Internet at http://pubs.acs.org.

References and Notes

(1) Barnes, A. M.; Bartle, K. D.; Thibon, V. R. A. *Tribol. Int.* **2001**, *34*, 389.
(2) Bartz, W. J. *Engine Oils and Automotive Lubrication*; Marcel Dekker: New York, 1993.
(3) Klamman, D., Ed. *Lubricants and Related Products*; Weinheim: Deerfield Beach, FL, 1984.
(4) Freuler, H. C. U.S. Patent 2,364,283, 1944.
(5) Kasrai, M.; Fuller, M.; Scaini, M.; Yin, Z.; Brunner, R. W.; Bancroft, G. M.; Fleet, M. E.; Fyfe, K.; Tan, K. H. In *Lubricants and Lubrication*; Dowson, D., Ed.; Elsevier: Amsterdam, 1995; p 659.
(6) Sarin, R.; Gupta, A. K.; Tuli, D. K.; Verma, A. S.; Rai, M. M.; Bhatnagar, A. K. *Tribol. Int.* **1993**, *26*, 389.
(7) Benchaita, M. T. *Lubr. Eng.* **1991**, *47*, 893.
(8) Harrison, P. G.; Brown, P. *Wear* **1991**, *148*, 123.
(9) Roby, S. H. *Lubr. Eng.* **1991**, *47*, 413.
(10) McGeehan, J. A.; Graham, J. P.; Yamaguchi, E. S. In *SAE 902162*; SAE: Warrendale, PA, 1990.
(11) Plaza, S. *ASLE Trans.* **1987**, *30*, 233.
(12) Dacre, B. H.; Bovington, C. *ASLE Trans.* **1981**, *24*, 546.
(13) Molina, A. *ASLE Trans.* **1979**, *30*, 479.
(14) Rounds, F. G. *ASLE Trans.* **1975**, *18*, 79.
(15) Lansdown, A. R. In *Chemistry and Technology of Lubricants*; Mortier, R. M., Orszulik, S. T., Eds.; Blackie: London, 1995.
(16) Yamaguchi, E. S. In *Proceedings of the Fourth International Symposium on the Performance Evaluation of Automotive Fuels and Lubricants*; CEC: Birmingham, UK, 1993; p 1.
(17) Atkary, M.; McDermott, M. T.; Torkelson, J. *Wear* **2001**, *247*, 172.
(18) Yin, Z.; Kasrai, M.; Fuller, M.; Bancroft, G. M.; Fyfe, K.; Tan, K. H. *Wear* **1997**, *202*, 172.
(19) Czichos, H. *Tribology: A Systems Approach*; Elsevier: Amsterdam, 1978.
(20) Roby, S. H.; Supp, J. A. In *SAE 952342*; SAE: Warrendale, PA, 1995.
(21) Korcek, S. In *Tribology 2000: 8th International Colloquium*; Bartz, W. J., Ed.; Technische Akademic Esslingen: Octfildem, 1992; Vol. 11, p 1-1 to 1-6.
(22) Wan, Y.; Cao, L.; Xue, Q. *Tribol. Int.* **1997**, *30*, 767.
(23) Schey, J. A.; Nautiyal, P. C. *Wear* **1991**, *37*, 146.
(24) Varlot, K.; Kasrai, M.; Martin, J. M.; Vacher, B.; Bancroft, G. M.; Yamaguchi, E. S.; Ryason, P. R. *Tribol. Lett.* **2000**, *8*, 9.
(25) Papay, A. G. *Lubr. Sci.* **1998**, *10*, 209.
(26) Willermet, P. A.; Pieprzak, J. M.; Dailey, D. P.; Carter, R. O., III.; Lindsay, N. E.; Haack, L. P.; DeVries, J. E. *ASLE Trans.* **1991**, *113*, 38.
(27) Bird, R. J.; Galvin, G. P. *Wear* **1976**, *37*, 143.
(28) Suominen Fuller, M. L.; Kasrai, M.; Bancroft, G. M.; Fyfe, K.; Tan, K. H. *Tribol. Int.* **1998**, *31*, 627.
(29) Willermet, P. A.; Dailey, D. P.; Carter, R. O., III.; Schmitz, P. J.; Zhu, W. *Tribol. Int.* **1995**, *28*, 177.
(30) Wu, Y. L.; Dacre, B. H. *Tribol. Int.* **1997**, *30*, 445.
(31) Willermet, P. A.; Dailey, D. P.; Carter, R. O., III.; Schmitz, P. J.; Zhu, W.; Bell, J. C.; Park, D. *Tribol. Int.* **1995**, *28*, 163.
(32) Barcroft, F. T.; Park, D. *Wear* **1986**, *108*, 213.
(33) Larsen, R. *Sci. Lubr.* **1958**, *10*, 12.
(34) Dickert, J. J.; Rowe, C. N. *J. Org. Chem.* **1967**, *32*, 647.
(35) Coy, R. C.; Jones, R. B. *ASLE Trans.* **1979**, *24*, 77.
(36) Jones, R. B.; Coy, R. C. *ASLE Trans.* **1979**, *24*, 91.
(37) Barcroft, F. T.; Bird, R. J.; Hutton, J. F.; Park, D. *Wear* **1982**, *77*, 355.
(38) Ashford, J. S.; Bretherick, L.; Gould, P. *J. Appl. Chem.* **1965**, *15*.
(39) Hanneman, W. W.; Porter, R. S. *J. Org. Chem.* **1964**, *29*, 2996.
(40) Spedding, H.; Watkins, R. C. *Tribol. Int.* **1982**, *15*, 9.
(41) Watkins, R. C. *Tribol. Int.* **1982**, *15*, 13.
(42) Armstrong, D. R.; Ferrari, E. S.; Roberts, K. J.; Adams, D. *Wear* **1997**, *208*, 138.
(43) Jiang, S.; Dasgupta, S.; Blanco, M.; Frazier, R.; Yamaguchi, E. S.; Tang, Y.; Goddard III, W. A. *J. Phys. Chem.* **1996**, *100*, 15760.
(44) Armstrong, D. R.; Ferrari, E. S.; Roberts, K. J.; Adams, D. *Wear* **1998**, *217*, 276.
(45) Jiang, S.; Frazier, R.; Yamaguchi, E. S.; Blanco, M.; Dasgupta, S.; Zhou, Y.; Tahir, C.; Tang, Y.; Goddard III, W. A. *J. Phys. Chem. B* **1997**, *101*, 7702.
(46) Zhou, Y.; Jiang, S.; Cagin, T.; Yamaguchi, E. S.; Frazier, R.; Ho, A.; Tang, Y.; Goddard III, W. A. *J. Phys. Chem. A* **2000**, *104*, 2508.
(47) Graham, J. F.; McCague, C.; Norton, P. R. *Tribol. Lett.* **1999**, *6*, 149.
(48) Fuller, M.; Yin, Z.; Kasrai, M.; Bancroft, G. M.; Yamaguchi, E. S.; Ryason, P. R.; Willermet, P. A.; Tan, K. H. *Tribol. Int.* **1997**, *30*, 305.
(49) Yamaguchi, E. S.; Ryason, P. R.; Labrador, E. Q.; Hansen, T. P. *Tribol. Int.* **1996**, *39*, 220.
(50) So, H.; Lin, Y. C.; Huang, G. G. S.; Chang, T. S. T. *Wear* **1993**, *166*, 17.

(51) Yin, Z.; Kasrai, M.; Bancroft, G. M.; Laycock, K. F.; Tan, K. H. *Tribol. Int.* **1993**, *20*, 383.
(52) Kohn, W.; Sham, L. J. *Phys. Rev. A* **1965**, *140*, 1133.
(53) Hohenburg, P.; Kohn, W. *Phys. Rev. B* **1964**, *136*, 864.
(54) te Velde, G.; Bickelhaupt, F. M.; van Gisbergen, S. J. A.; Fonseca Guerra, C.; Baerends, E. J.; Snijders, J. G.; Ziegler, T. *J. Comput. Chem.* **2001**, *22*, 931.
(55) Fonseca Guerra, C.; Snijders, J. G.; te Velde, G.; Baerends, E. J. *Theor. Chem. Acc.* **1998**, *99*, 391.
(56) Baerends, E. J.; Autschbach, J. A.; Berces, A.; Bo, C.; Boerrigter, P. M.; Cavallo, L.; Chong, D. P.; Deng, L.; Dickson, R. M.; Ellis, D. E.; Fan, L.; Fischer, T. H.; Fonseca Guerra, C.; van Gisbergen, S. J. A.; Groeneveld, J. A.; Gritsenko, O. V.; Gruning, M.; Harris, F. E.; van den Hoek, P.; Jacobsen, H.; van Kessel, G.; Kootstra, F.; van Lenthe, E.; Osinga, V. P.; Patchkovskii, S.; Philipsen, P. H. T.; Post, D.; Pye, C. C.; Ravenek, W.; Ros, P.; Schipper, P. R. T.; Schreckenback, G.; Snijders, J. G.; Sola, M.; Swart, M.; Swerhone, D.; te Velde, G.; Vernooijs, P.; Versluis, L.; Visser, O.; van Wezenbeek, E.; Wiesenekker, G.; Wolff, S. K.; Woo, T. K.; Ziegler, T. *ADF*, version 2001.01; Scientific Computing and Modelling NV: Amsterdam, The Netherlands, 2002.
(57) Perdew, J. P.; Burke, K.; Ernzerhof, M. *Phys. Rev. Lett.* **1996**, *77*, 3865.
(58) Zhang, Y.; Yang, W. *Phys. Rev. Lett.* **1998**, *80*, 890.
(59) Vosko, S. H.; Wilk, L.; Nusair, M. *Can. J. Phys.* **1980**, *58*, 1200.
(60) Mayo, S. L.; Olafson, B. D.; Goddard III, W. A. *J. Phys. Chem.* **1990**, *94*, 8897.
(61) Molecular Simulations Inc.: San Diego, 1999.
(62) Frisch, M. J.; Trucks, G. W.; Schegel, H. B.; Scuseria, G. E.; Robb, M. A.; Cheeseman, J. R.; Zakrewski, V. G.; Montgomery, J., J. A.; Stratmann, R. E.; Burant, J. C.; Dapprich, S.; Millam, J. M.; Daniels, A. D.; Kudin, K. N.; Strain, M. C.; Farkas, O.; Tomasi, J.; Barone, V.; Cossi, M.; Cammi, R.; Mennucci, B.; Pomelli, C.; Adamo, C.; Clifford, S.; Ochterski, J.; Petersson, G. A.; Ayala, P. Y.; Cui, Q.; Morokuma, K.; Malick, D. K.; Rabuck, A. D.; Raghavachari, K.; Foresman, J. B.; Cioslowski, J.; Ortiz, J. V.; Baboul, A. G.; Stefanov, B. B.; Liu, G.; Liashenko, A.; Piskorz, P.; Komaromi, I.; Comperts, R.; Martin, R. L.; Fox, D. J.; Keith, T.; Al-Laham, M. A.; Peng, C. Y.; Nanayakkara, A.; Gonzalez, C.; Challacombe, M.; Gill, P. M. W.; Johnson, B. G.; Chen, W.; Wong, M. W.; Andres, J. L.; Head-Gordon, M.; Replogle, E. S.; Pople, J. A. *Gaussian98*; Gaussian, Inc.: Pittsburgh, PA, 1998.
(63) Stewart, J. J. P. *J. Comput. Chem.* **1989**, *10*, 209.
(64) Stewart, J. J. P. *J. Comput. Chem.* **1989**, *10*, 221.
(65) Car, R.; Parinello, M. *Phys. Rev. Lett.* **1985**, *55*, 2471.
(66) Hutter, J.; Alavi, A.; Deutsch, T.; Bernasconi, M.; Goedecker, S.; Marx, D.; Tuckerman, M.; Parinello, M. *CPMD*, version 3.5; MPI für Festkorperforschung and IBM Zurich Research Laboratory: Zurich, Switzerland, 1995−1999.
(67) Hartswigsen, C.; Goedecker, S.; Hutter, J. *Phys. Rev. B* **1998**, *58*, 3641.
(68) Goedecker, S.; Teter, M.; Hutter, J. *Phys. Rev. B* **1996**, *54*, 1703.
(69) Matveev, A.; Staufer, M.; Mayer, M.; Rösch, N. *Int. J. Quantum Chem.* **1999**, *75*, 863.
(70) Hammer, B.; Hansen, L. B.; Norskov, J. K. *Phys. Rev. B* **1999**, *59*, 7413.
(71) Harrison, P. G.; Brown, P.; McManus, J. *Inorg. Chim. Acta* **1992**, *202*, 3.
(72) Harrison, P. G.; Brown, P.; Hynes, M. J.; Kiely, J. M.; McManus, J. *J. Chem. Res., Synop.* **1991**, 174.
(73) Harrison, P. G.; Sebald, A. *J. Chem. Res., Synop.* **1991**, 340.
(74) Lawton, S. L.; Kokotailo, G. T. *Inorg. Chem.* **1969**, *8*, 2410.
(75) Ito, T.; Igarashi, T.; Hitosi, H. *Acta Crystallogr., Sect. B* **1969**, *B25*, 2303.

(76) For comparison the dimerization energy of the H-substituted ZDDP was determined to be −9.9 kcal/mol through geometry optimizations performed with CPMD and the PBE functional. Although this is lower than the revPBE/TZP dimerization energy calculated with ADF, it is in good agreement with the PBE/TZP dimerization energy of −11.9 kcal/mol calculated with ADF.

(77) It was found that the accumulation of attractive dispersion forces not accounted for by DFT became significant in the calculation of the dimerization energies. Correcting the dimerization energies for these forces with the attractive component of a Lennard-Jones potential within the Dreiding force field[60] decreased the dimerization energies in all cases. The corrected energies are −17.1, −7.6, −1.3, 2.6, 3.1, and 14.5 kcal/mol for the H-, Me-, Et-, ^{i}Pr-, ^{t}Bu-, and Ph-substituted species, respectively. This shows that with these attractive dispersion forces there is an increase in the relative stability of the dimer; however, for ZDDPs with large substituents, which are typical of those used in motor oils, the monomer is still favored. Furthermore, at finite temperature entropic contributions to the free energy will increase the energetic favorability of the monomer. Thus, although the dimerization energies are changed when attractive dispersion forces are taken into account, the inclusion of these additional energy terms does not affect the general conclusions presented in the text.

(78) Gallopoulos, N. E. *Am. Chem. Soc., Div. Petrol. Chem., Prepr.* **1966**, *11*, 21.
(79) Heilweil, I. J. *Am. Chem. Soc., Div. Petrol. Chem., Prepr.* **1965**, *10*, D-19.
(80) Harrison, P. G.; Kikabhai, T. *Wear* **1987**, *116*, 25.
(81) Dacre, B. H.; Bovington, C. *ASLE Trans.* **1983**, *25*, 546.
(82) Dacre, B. H.; Bovington, C. *ASLE Trans.* **1983**, *26*, 33.
(83) Madelung, O.; Schulz, M.; Weiss, H. *Numerical Data and Functional Relationships in Science and Technology, Group III*; Springer-Verlag: Berlin, 1982; Vol. 17(b).